Supplement of Biogeosciences, 22, 4187–4201, 2025
https://doi.org/10.5194/bg-22-4187-2025-supplement


Biogeosciences Open Access EGU

*Supplement of*

# Southern Hemisphere tree rings as proxies to reconstruct Southern Ocean upwelling

**Christian Lewis et al.**

*Correspondence to:* Christian Lewis (c.lewis@gns.cri.nz)

## S1. Methods: Further explanation of the Monte Carlo scheme to estimate uncertainties in data interpolation

All tree-ring $\Delta^{14}C$ measurements are associated with dates centered in the summer of the growth season (i.e., for a tree growing between Southern Hemisphere spring to Autumn, September to May for example, the midpoint is peak summer; January 1). We want these measurements to be contextualized by the Southern Hemisphere Background (SHB) reference, a combination of two long-term records originating from University of Heidelberg's Cape Grim station, and GNS/NIWA Baring Head station. However, in order to find the difference between tree-ring $\Delta^{14}C$ and the SHB, the temporal axes need to be matched.

To achieve this, we smooth the SHB using use the NOAA Global Monitoring Laboratory's CCGCRV curve fitting method (Thoning et al., 1989), setting the algorithm to output data to match a concatenated list of the SHB collection dates and tree-ring dates. Both the "smooth" and "trend" functions are employed, however, only the "trend" function output is used in the final manuscript. To estimate the uncertainty the output, smoothed SHB, the CCGCRV algorithm is run inside a Monte Carlo loop. It proceeds as follows (line numbers refer to X_my_function.py; https://github.com/christianlewis091/science_projects/blob/main/SOAR_Tree_rings/scripts_OPEN_ACCESS/X_my_functions.py:)

1. Initial data is fed into the loop, including a) SHB x-values, b) x-values where output will be assigned (the concatenated SHB and tree-ring x-values), c) SHB y-values ($\Delta^{14}C$, ‰) d) SHB y-value error ($\Delta^{14}C$, ‰), e) parameterization of the FFT cutoff, d) times to loop (10k).
2. The first for-loop (lines 311-326):
    a. Iterate through the y-values (SHB $\Delta^{14}C$'s), and randomly return a value within the normal distribution of that y-value's error-range.
    b. Create "n" (10,000) sets of the randomized SHB, all stacked up
3. Second for-loop (lines 338-341):
    a. Iterate through the stack (array) from the previous loop (each iteration is a randomized SHB, referred to below as "sub-SHB")
    b. Run the sub-SHB through ccgFilter (line 340).
    c. Save the smoothed-output in a vertical stack (line 341).
4. Third for-loop (lines 354-364):
    a. For each x-value, find the mean and standard deviation of the smoothed outputs (a mean and standard deviation for smoothed y-values for each individual x-value in time). This is the value used for the remainder of analysis.

## S2. Methods: Tree-ring validation and figures

Ensuring that tree-rings are counted properly for correct chronologies is critical. This is described in the final paragraph of the main manuscript section 2.1. Below are figures used for ring-count validation for each site. Additional per-site information and descriptions are in figure captions.

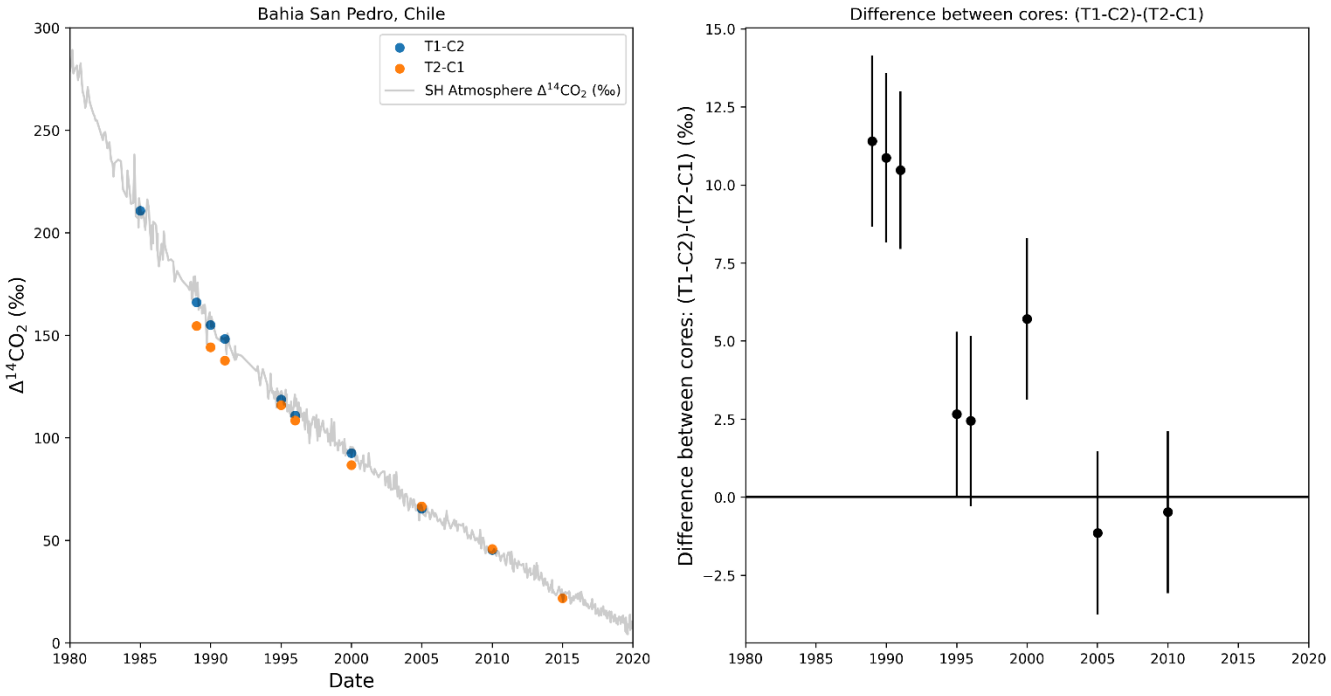


**Fig. S1. The Bahia San Pedro record includes two trees, each with multiple cores. The second core from Tree 1 and first core from Tree 2 were chosen for measurement. The two records deviate from each other before 2005, therefore, all data before 2005 has been removed from the analysis.**

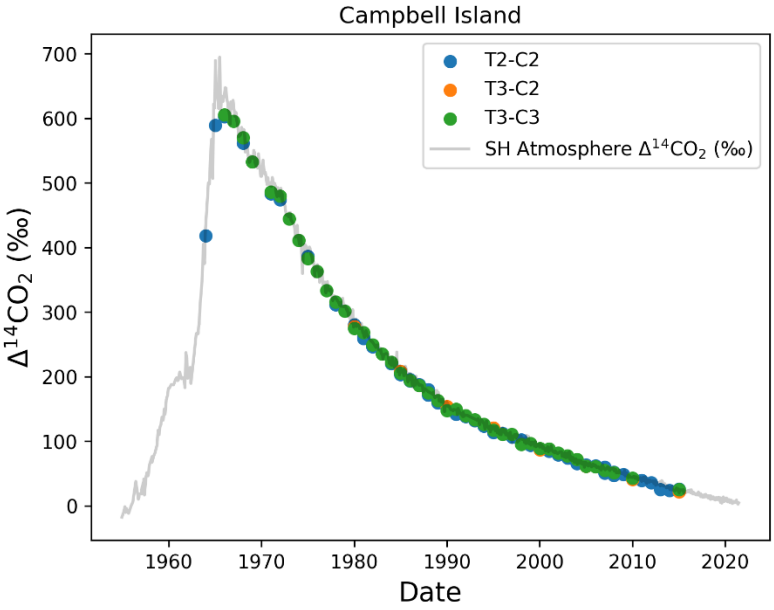


**Fig. S2.** No data was removed from Campbell Island Record.

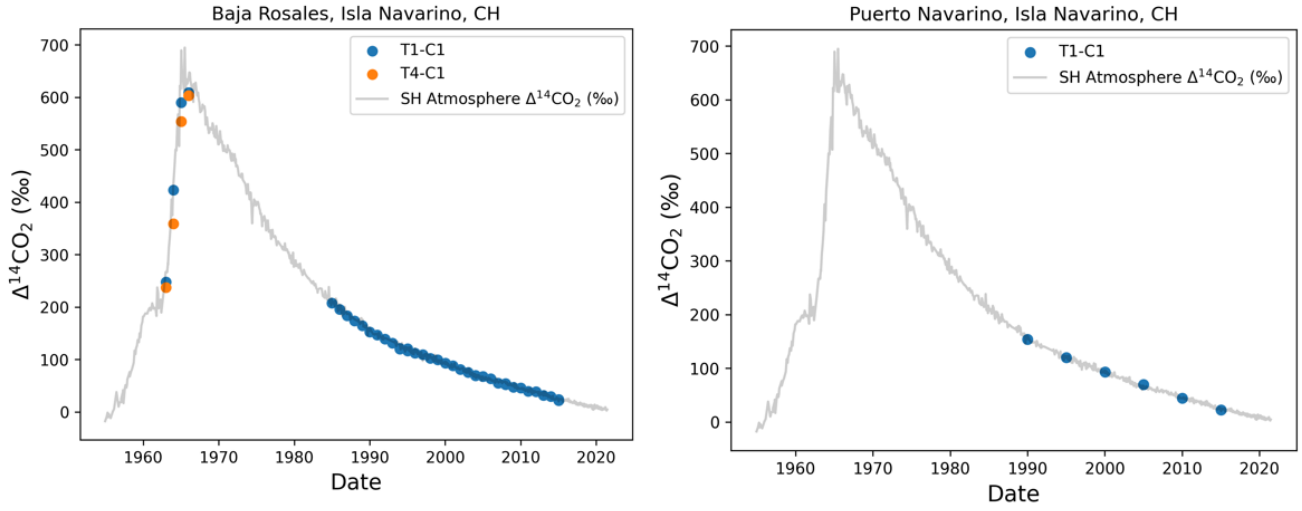


**Fig. S3. Of the two neighboring sites, Puerto Navarino lies further west and is in proximity to the Argentinian city of Ushuaia, while Baja Rosales is to the east. These two sites were selected with the expectation that any significant land biosphere signal or fossil fuel emissions from urban influence would lead to measurable differences between the two sites however, no statistically significant offset is found between them (see Figure S13).**

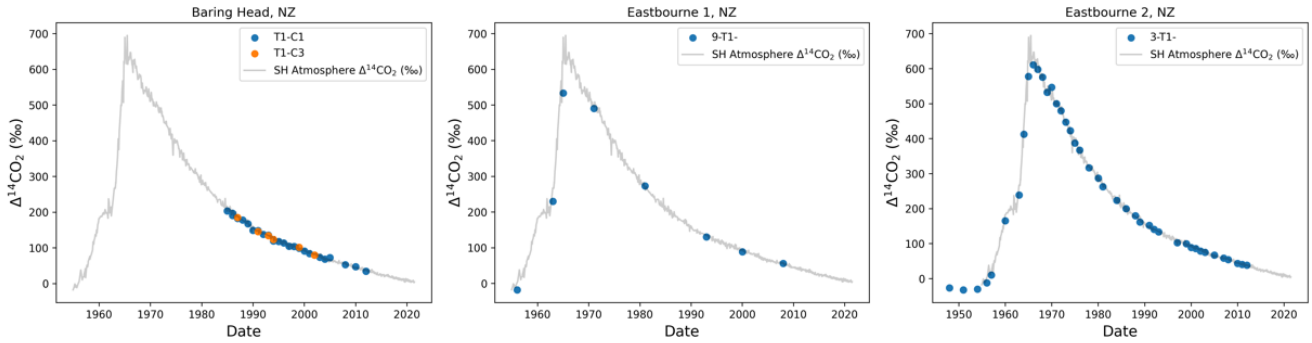


**Fig. S4.** Baring Head and Eastbourne sites (Turnbull et al., 2017):
No data were removed from any of these sites during ring-count validations. The Baring Head pine is 10m from the 14C sampling station, and on the clifftop exposed to oceanic air. The Eastbourne trees are 15 km from Baring Head, on Wellington Harbor.

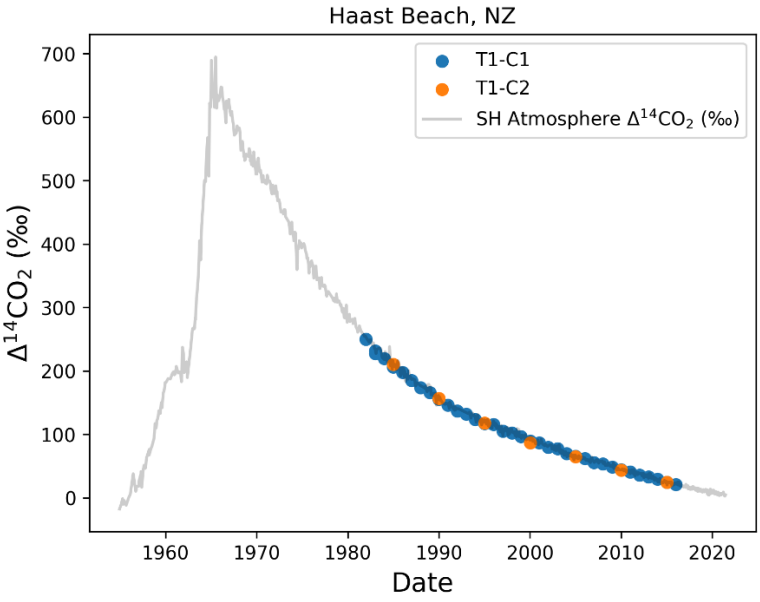


**Fig. S5. No data were removed during ring-count validation**.

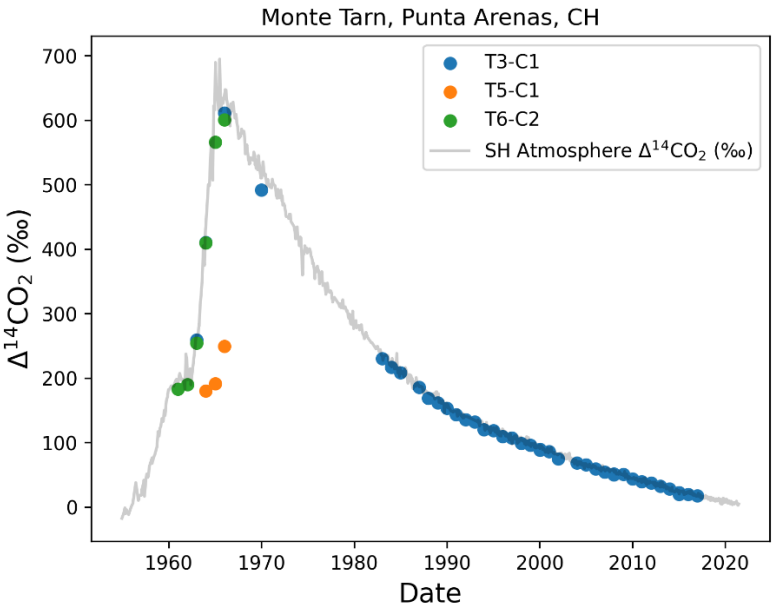


**Fig. S6. Tree 5, Core 1 was removed because it does not match the bomb spike**

100

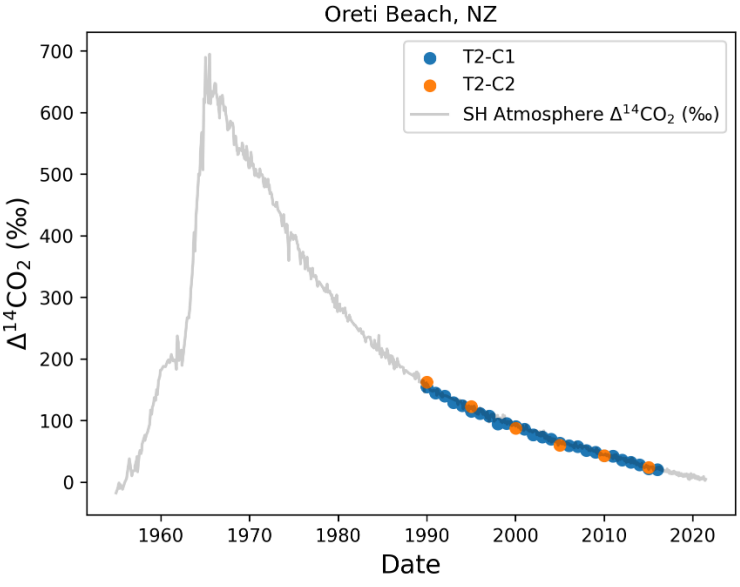

**Fig. S7. Cores from Oreti Beach agree as far back as 2000 and then the 1995 and 1990 pairs diverge indicating a ring count error in one or other core. All samples from 1999 back are therefore suspect and are not used.**

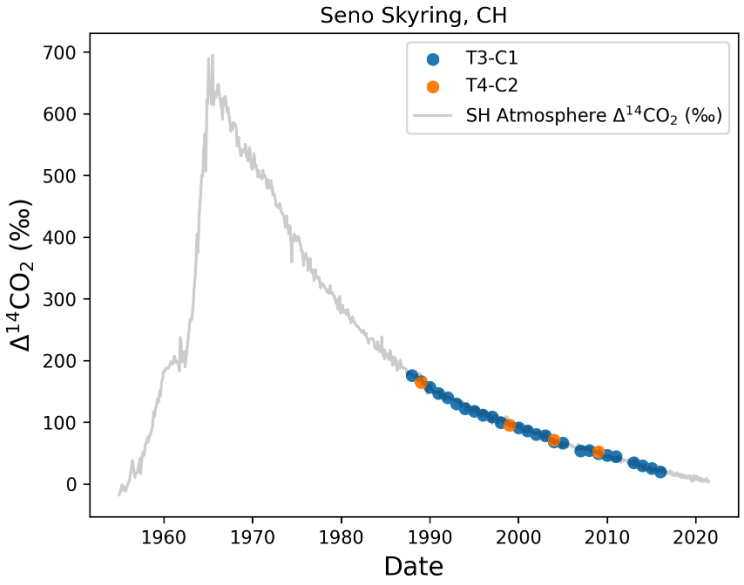


**Fig. S8. No data removed from this site**

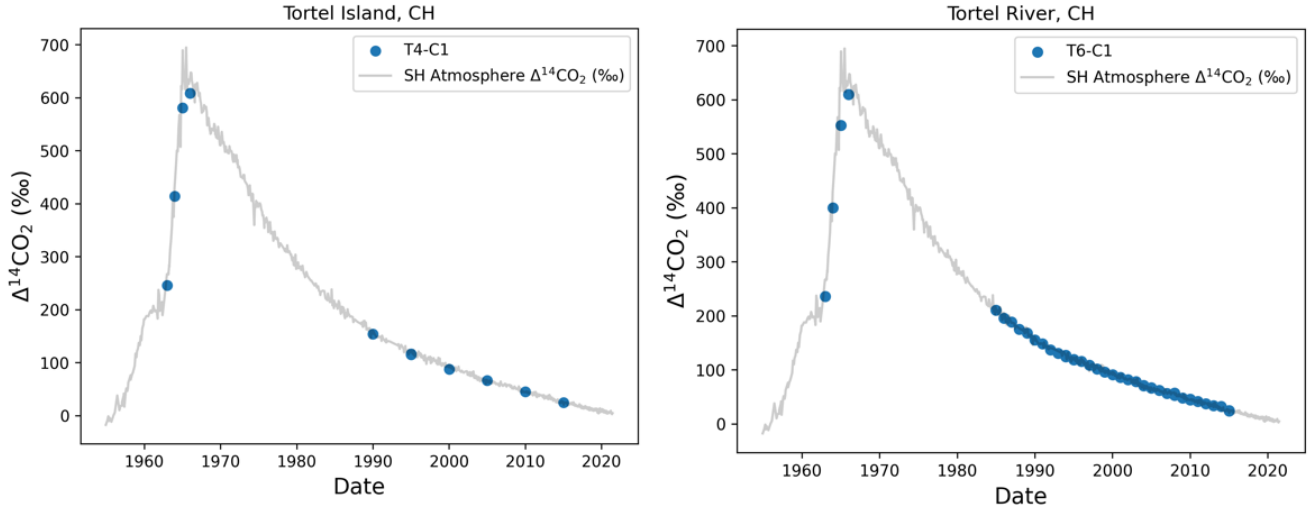


**Fig. S9. No data removed from these sites.**

## S3. Results: Additional versions of Figure 3.

Fig. 3 in the main text shows the mean $\Delta\Delta^{14}CO_2$ value for each site. It is useful to visualize the individual data overlaid upon the mean (Fig S10). Error bars represent 1 standard deviation from the mean. Figures S11 and S12 add descriptive statistics to the figure. Figure S11 shows statistics and 95% confidence interval calculated for all $\Delta\Delta^{14}CO_2$ values. Figure S11 shows the same but for mean $\Delta\Delta^{14}CO_2$ values.

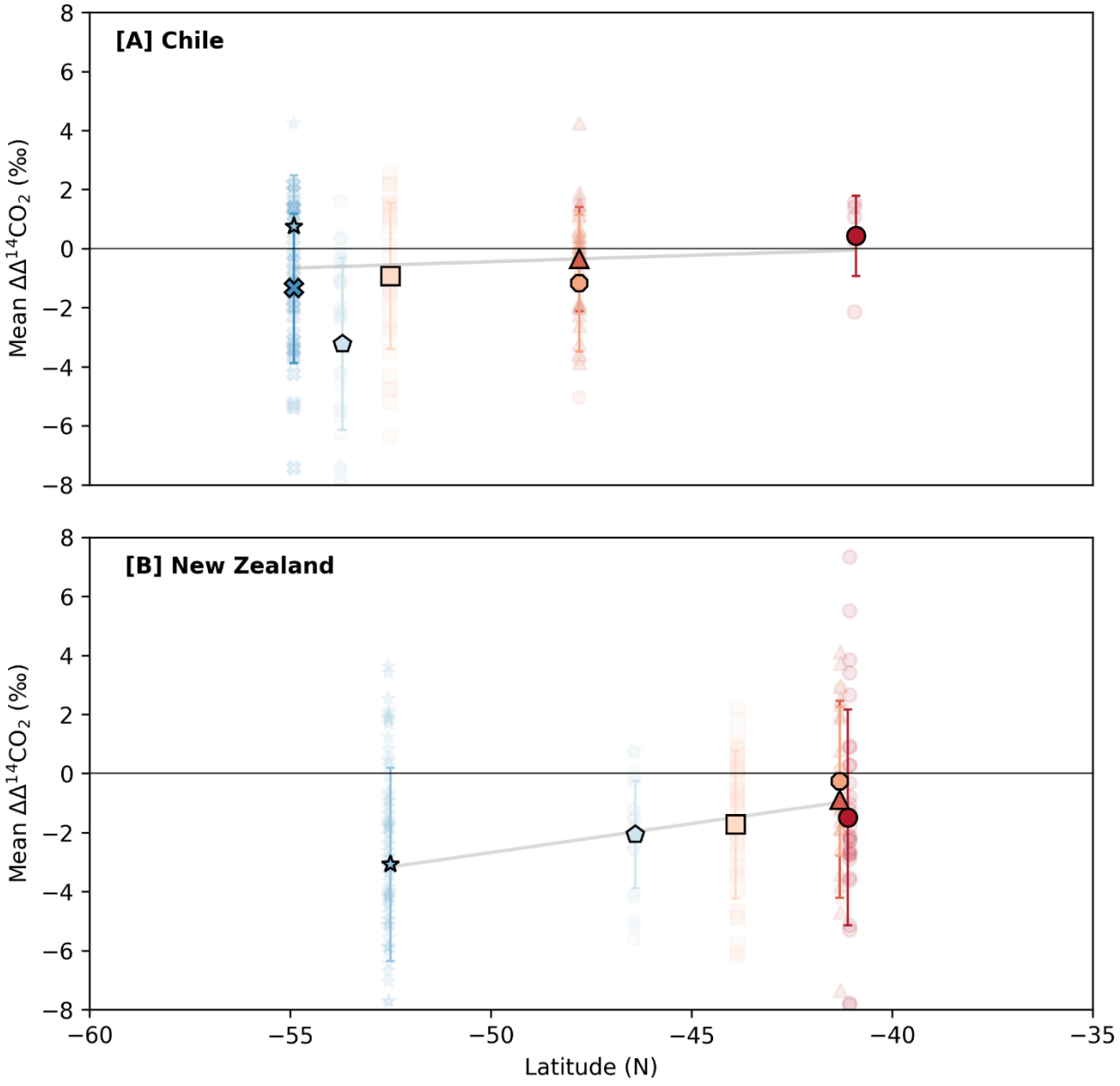


**Fig S10. A repeat of manuscript Fig. 3 but overlaid with the individual $\Delta\Delta^{14}CO_2$ values behind each site mean.**

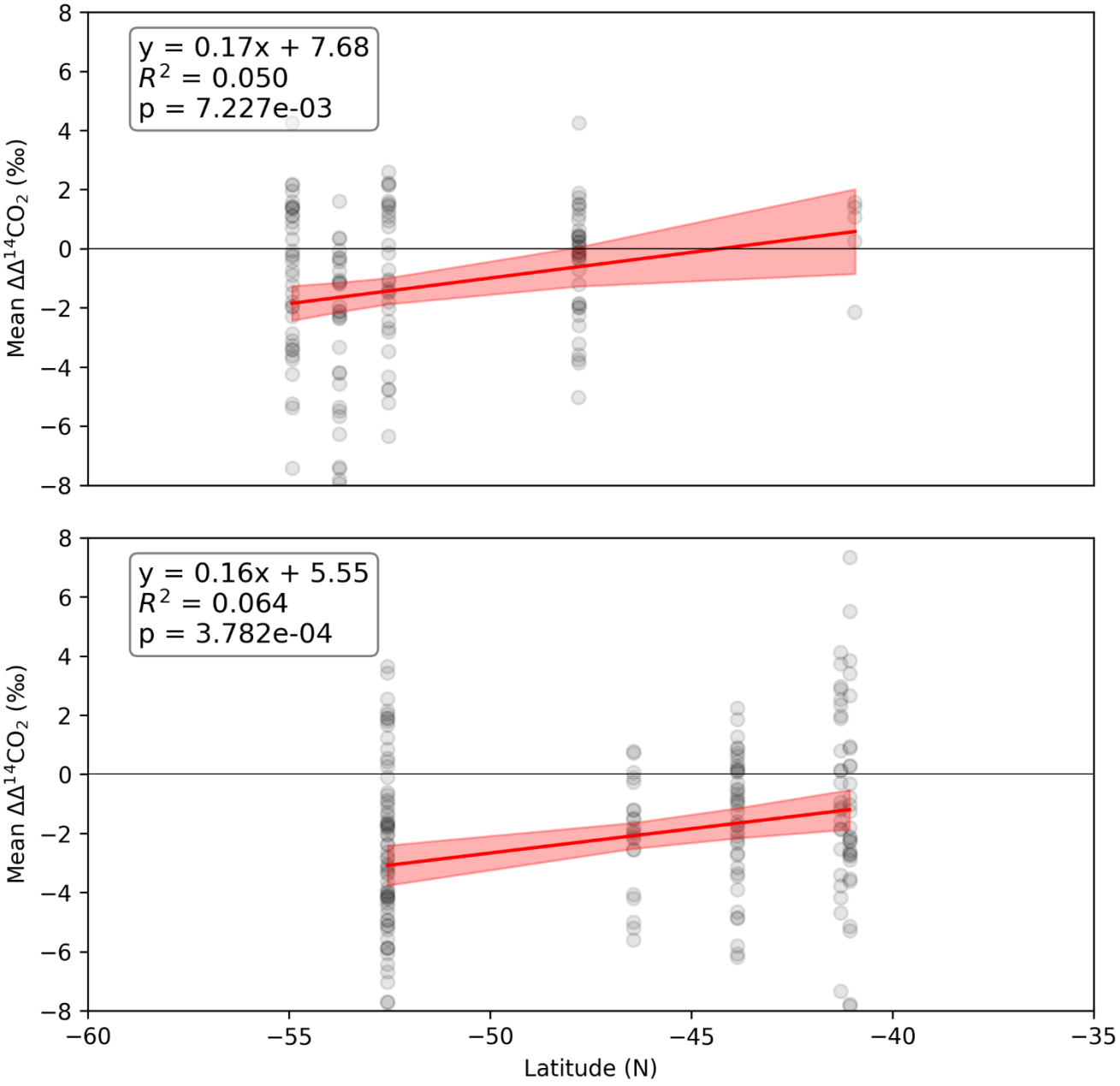


**Fig S11. Statistics overlaid on a plot of $\Delta\Delta^{14}CO_2$ versus latitude for Chile (top) and New Zealand (bottom).**

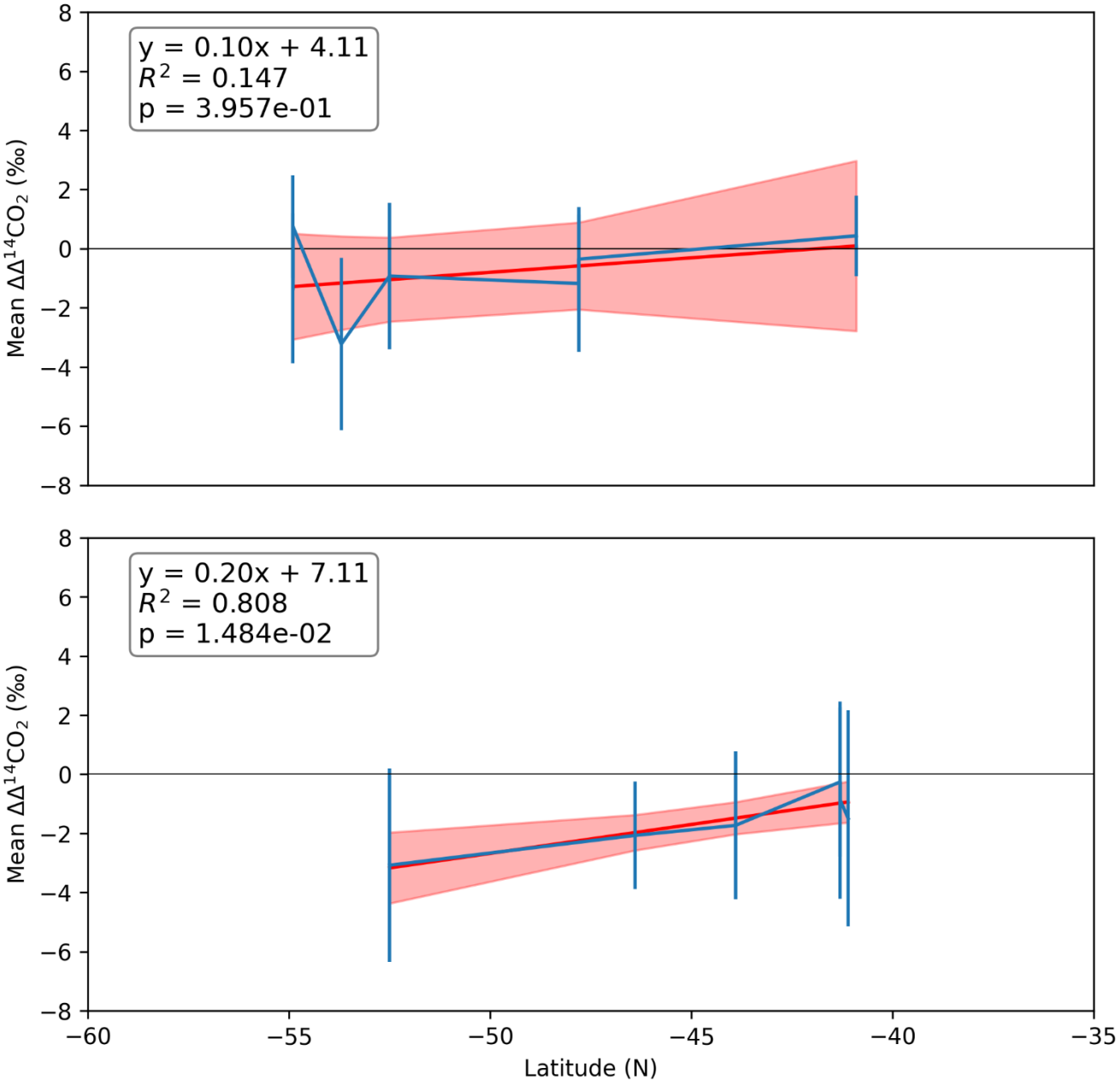


**Fig S12. Statistics overlaid on a plot of mean $\Delta\Delta^{14}CO_2$ versus latitude for Chile (top) and New Zealand (bottom).**

**S4. Exploration of a difference between two sites on Isla Navarino, Chile**

All tree-ring sites were selected on the west coast of land masses to ensure that sites saw prevailing westerly winds with no potential fossil or biospheric influences upstream. In the case of Puerto Navarino and Baja Rosales, both were sampled in an attempt to understand if trees would capture fossil $CO_2$ signal at the site down winds of Ushuaia, Argentina. Such a signal would manifest in lower values found at Baja Rosales. Baja Rosales mean $\Delta\Delta^{14}CO_2$ is 1.3 ± 2.5, while Puerto Navarino is 0.8 ± 1.7. An independent t-test shows the data are not different (p=0.06).

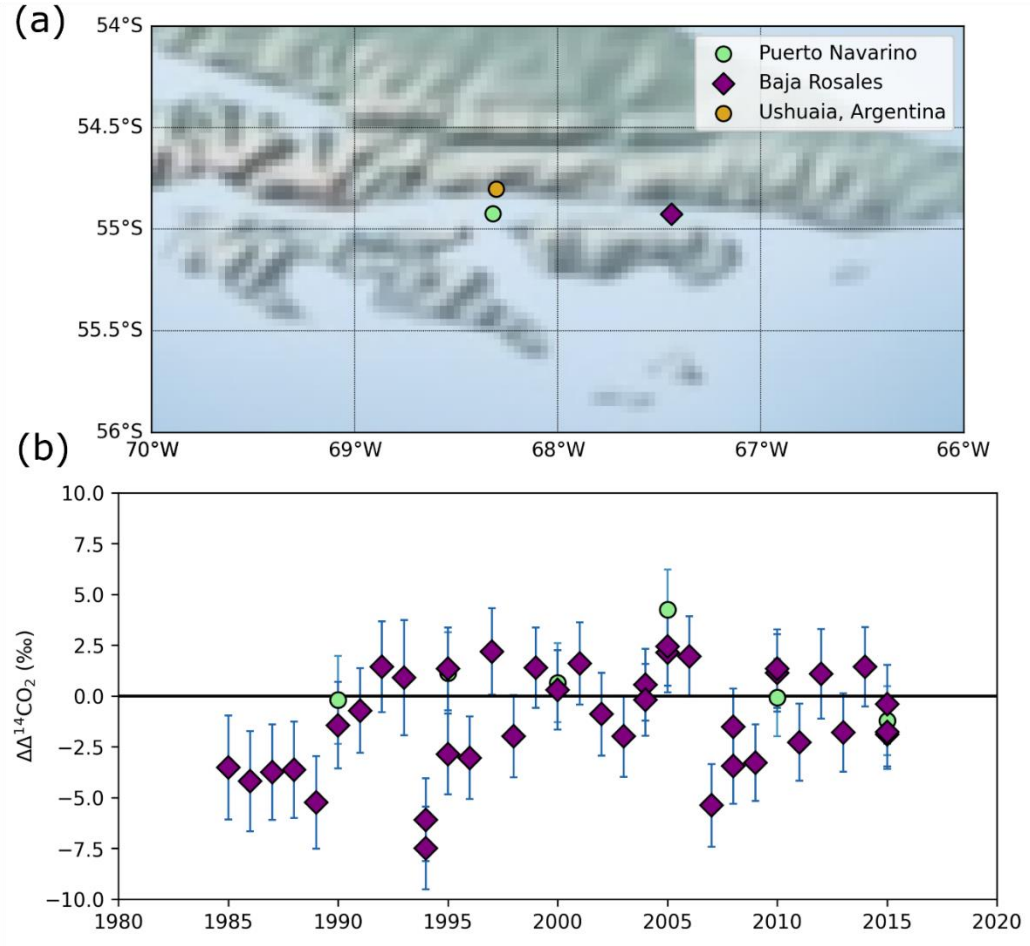


**Fig. S13. $\Delta\Delta^{14}CO_2$ of Puerto Navarino and Baja Rosales. An independent t-test yields a p-value of 0.07, which is too high to reject the null-hypothesis that the data are not different.**

**S5. Discussion of GLODAP and HYSPLIT data analysis**

Analysis of the GLODAP and HYSPLIT both required the interpolation of Southern Ocean front data (Orsi et al., 1995; Freeman and Lovenduski, 2016) to longitude values consistent with a) the GLODAP DIC $\Delta^{14}C$ measurements and 2) HYSPLIT back trajectory data points. In other words, to know if a GLODAP $\Delta^{14}C$ data-point, or a HYSPLIT back-trajectory temporal snapshot is in the Antarctic Southern Zone, I must know the latitudes of those fronts at the exact longitude to compute it's "region".

The interpolation was performed using the "numpy.interp" function, and was verified to be well-constructed by visually looking at the interpolation over the original fronts. This can be seen **Fig S14**, with dotted lines showing fronts, and red scattered points showing the interpolated front at a new given longitude.

After interpolations shown in Supplementary Figure 1 were complete, data was parsed into different Southern Ocean zones by comparing the actual latitude to frontal latitudes. This was verified to be working by visual inspection. Examples of parsed GLODAP and HYSPLIT outputs are shown in **Fig S15.** After verification of successful binning, the data can be averaged more easily using python's pandas library.

These codes can be found below. For HYSPLIT code, see HYSPLIT_check_Dec3_2024.py. For GLODAP code see, GLODA_check_Nov29_2024. The final data can be found in the "HYSPLIT" and "GLODAP" tabs of the associated data file.

https://github.com/christianlewis091/science_projects/tree/main/soar_tree_rings/scripts_EGU_submission

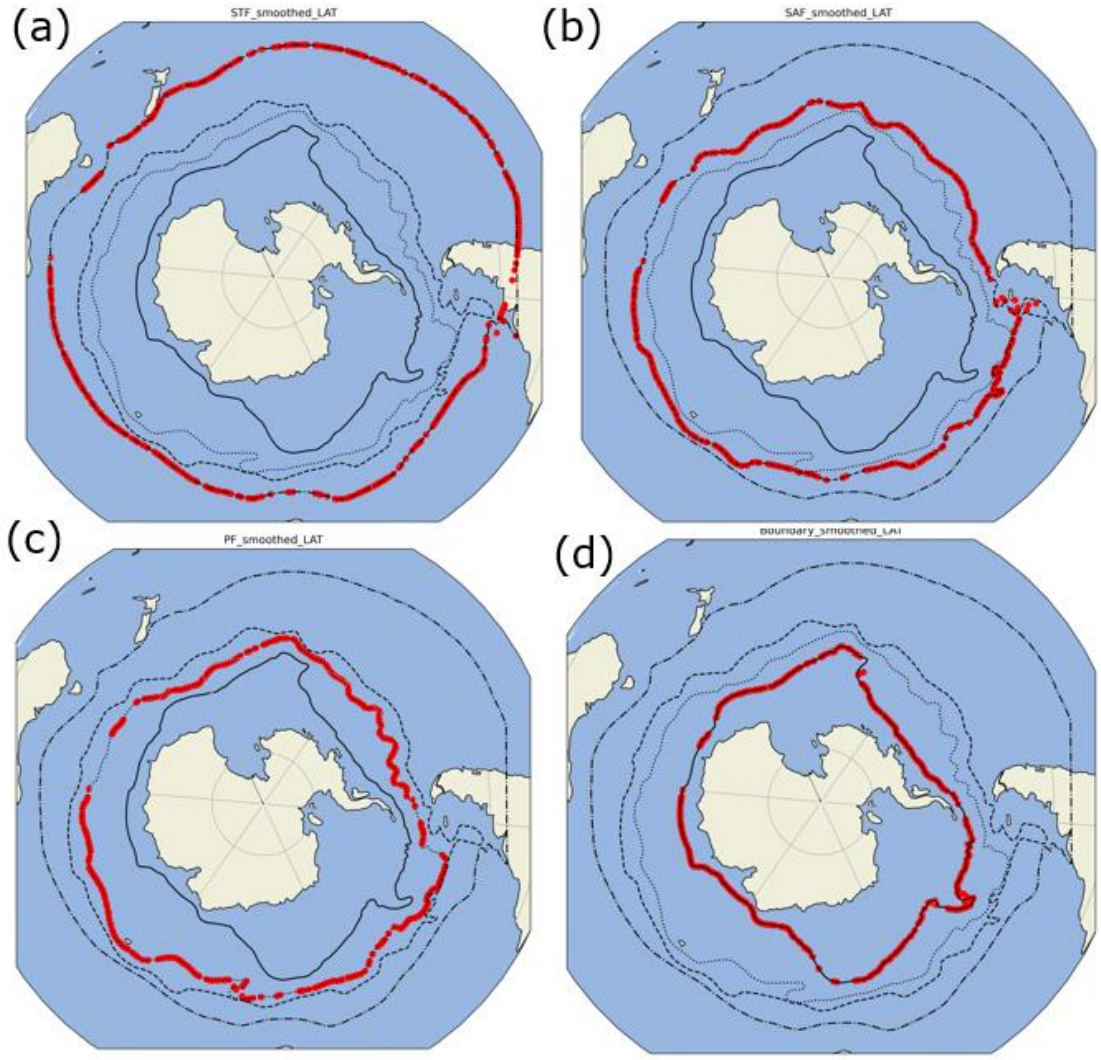


**Fig. S14. (Orsi, 1995) fronts (dotted lines) overlaid with interpolated front at a new given longitude (red scattered points). The scattered data represent longitudes of GLODAP surface ocean DIC $\Delta^{14}C$ measurements**

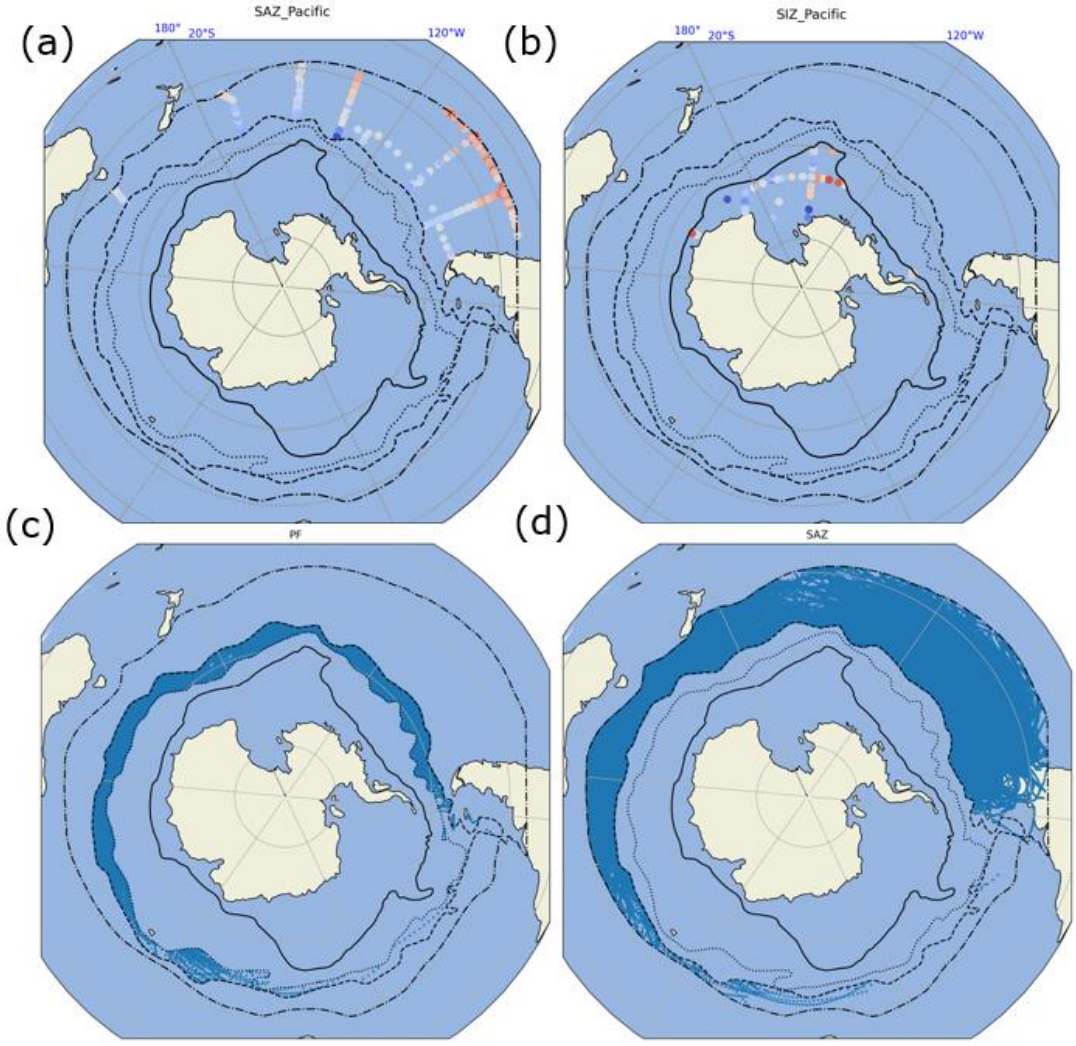


**Fig. S15. Examples of visual verification that data has been properly binned between the Southern Ocean frontal zones. A) and B) show GLODAP measurements binned to the Subantarctic Zone (SAZ) and the Seasonal Ice Zone (SIZ), respectively. C) and D) show HYSPLIT output binned into the Polar Frontal Zone (PFZ) and Subantarctic Zone (SAZ). Remaining examples added to Supplementary_Figures.pptx**

**S6. Remaining HYSPLIT back-trajectories**

Below, all HYSPLIT back-trajectory heat maps are shown. Only a sub-set of 4 sites are shown in the main text.

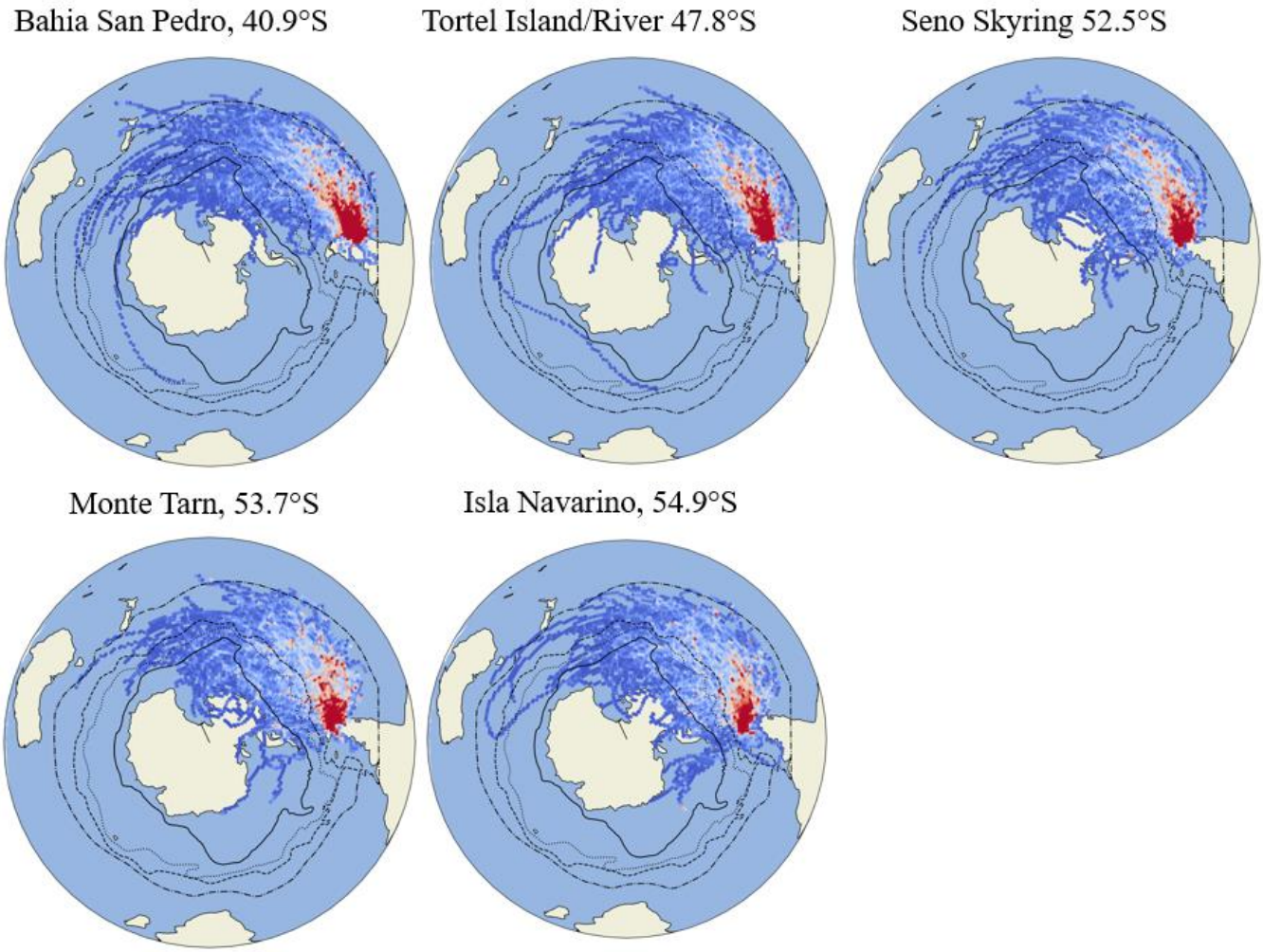


**Fig. S13. HYSPLIT back-trajectory heatmaps for sites in Chile.**

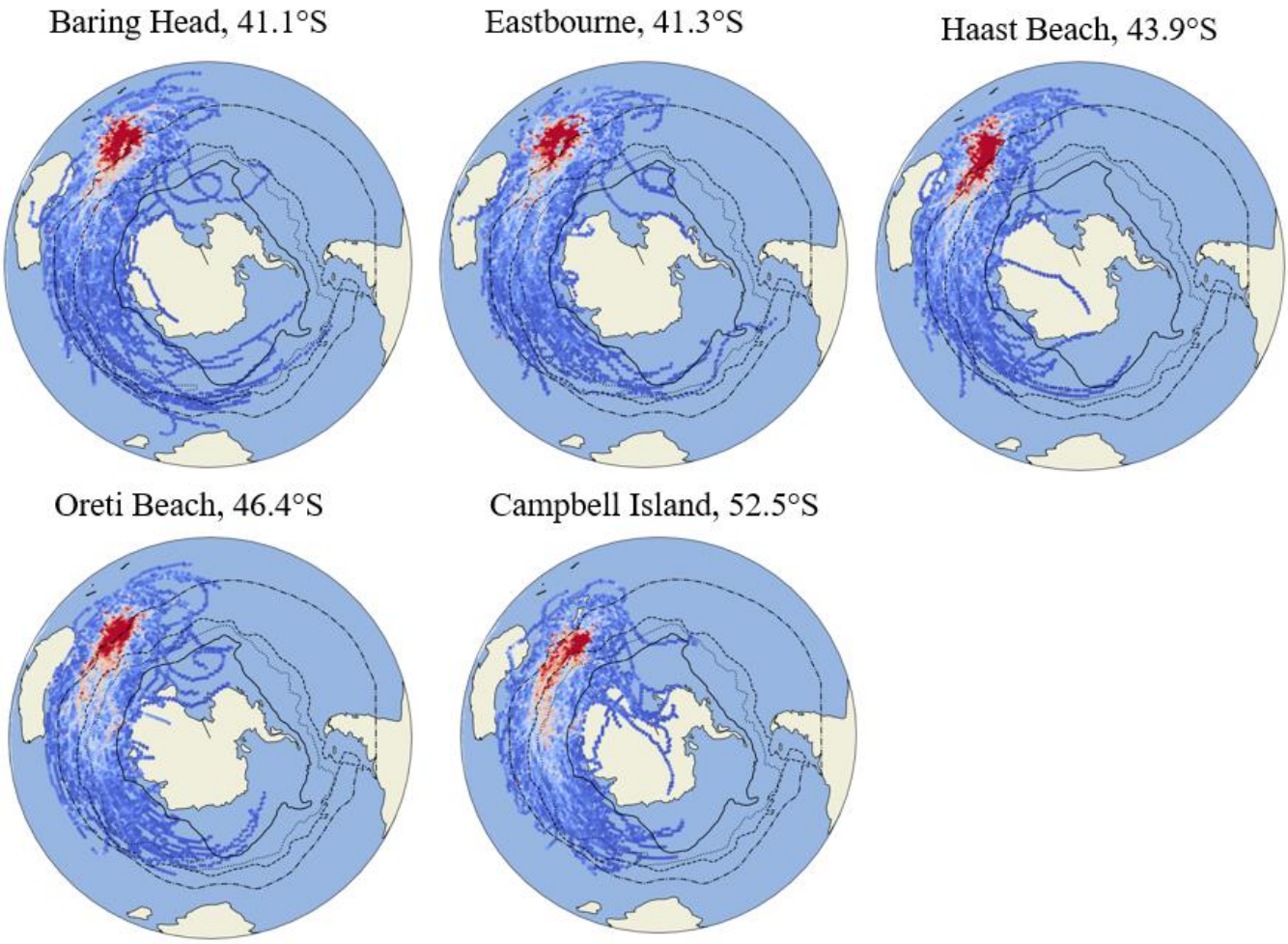


**Fig. S14. HYSPLIT back-trajectory heatmaps for sites in New Zealand.**

## S7. Comparison of Campbell Island record with other Southern Hemisphere $^{14}C$ records

In manuscript section 3.1, we discuss how the tree-ring $^{14}C$ measurements presented compare with other Southern Hemisphere $^{14}C$ datasets. Please refer to that section for a full description. Campbell Island record disagrees with another Campbell Island record (Turney et al, 2018) but agrees with atmospheric records from nearby Macquarie Island, and Neumayer Station.

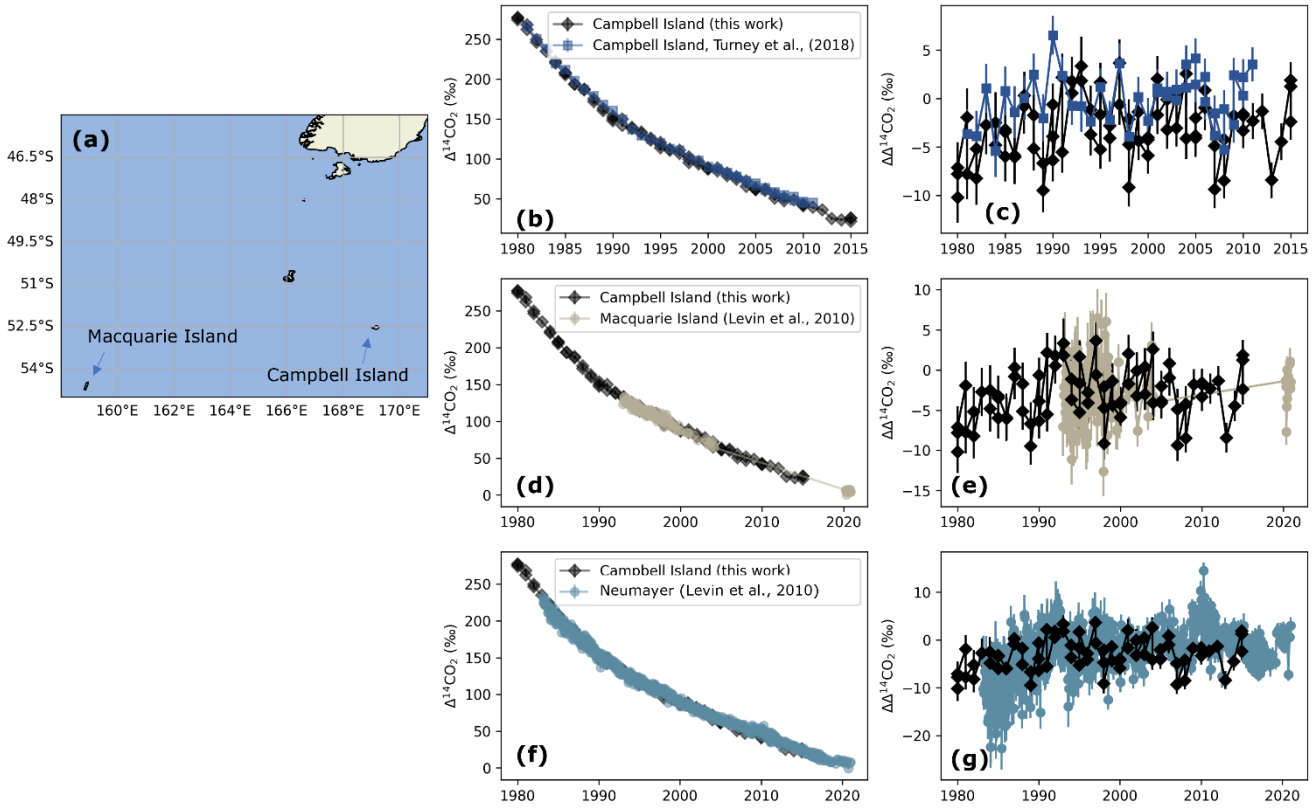


**Fig. S15. (A) Map showing the proximity of Campbell Island to Macquarie Island. (B, D, F) compare the $\Delta^{14}CO_2$ of our Campbell Island tree-ring measurements, and that of (Turney et al., 2018), and Macquarie Island and Neumayer Station from Levin et al., (2010). (C, E, and G) compare respective $\Delta\Delta^{14}CO_2$**